



FKA-Owl: Advancing Multimodal Fake News Detection through Knowledge-Augmented LVLMS

Xuannan Liu
Beijing University of Posts and
Telecommunications
liuxuannan@bupt.edu.cn

Peipei Li*
Beijing University of Posts and
Telecommunications
lipei@bupt.edu.cn

Huaibo Huang
Institute of Automation, Chinese
Academy of Sciences
huaibo.huang@cripac.ia.ac.cn

Zekun Li
University of California, Santa
Barbara
zekunli@cs.ucsb.edu

Xing Cui
Beijing University of Posts and
Telecommunications
cuixing@bupt.edu.cn

Jiahao Liang
Beijing University of Posts and
Telecommunications
jiahao.liang@bupt.edu.cn

Lixiong Qin
Beijing University of Posts and
Telecommunications
lxqin@bupt.edu.cn

Weihong Deng
Beijing University of Posts and
Telecommunications
whdeng@bupt.edu.cn

Zhaofeng He
Beijing University of Posts and
Telecommunications
zhaofenghe@bupt.edu.cn

Abstract

The massive generation of multimodal fake news involving both text and images exhibits substantial distribution discrepancies, prompting the need for generalized detectors. However, the insulated nature of training restricts the capability of classical detectors to obtain open-world facts. While Large Vision-Language Models (LVLMS) have encoded rich world knowledge, they are not inherently tailored for combating fake news and struggle to comprehend local forgery details. In this paper, we propose FKA-Owl, a novel framework that leverages forgery-specific knowledge to augment LVLMS, enabling them to reason about manipulations effectively. The augmented forgery-specific knowledge includes semantic correlation between text and images, and artifact trace in image manipulation. To inject these two kinds of knowledge into the LVLMS, we design two specialized modules to establish their representations, respectively. The encoded knowledge embeddings are then incorporated into LVLMS. Extensive experiments on the public benchmark demonstrate that FKA-Owl achieves superior cross-domain performance compared to previous methods. Code is publicly available at https://liuxuannan.github.io/FKA_Owl.github.io/.

CCS Concepts

• **Security and privacy** → **Social aspects of security and privacy**; • **Information systems** → *Multimedia information systems*.

* Corresponding author.

Permission to make digital or hard copies of all or part of this work for personal or classroom use is granted without fee provided that copies are not made or distributed for profit or commercial advantage and that copies bear this notice and the full citation on the first page. Copyrights for components of this work owned by others than the author(s) must be honored. Abstracting with credit is permitted. To copy otherwise, or republish, to post on servers or to redistribute to lists, requires prior specific permission and/or a fee. Request permissions from permissions@acm.org.
MM '24, October 28–November 1, 2024, Melbourne, VIC, Australia
© 2024 Copyright held by the owner/author(s). Publication rights licensed to ACM.
ACM ISBN 979-8-4007-0686-8/24/10
<https://doi.org/10.1145/3664647.3681089>

Keywords

Multimodal Fake News Detection, Large Vision-Language Model, Knowledge Augmentation

ACM Reference Format:

Xuannan Liu, Peipei Li, Huaibo Huang, Zekun Li, Xing Cui, Jiahao Liang, Lixiong Qin, Weihong Deng, and Zhaofeng He. 2024. FKA-Owl: Advancing Multimodal Fake News Detection through Knowledge-Augmented LVLMS. In *Proceedings of the 32nd ACM International Conference on Multimedia (MM '24)*, October 28–November 1, 2024, Melbourne, VIC, Australia. ACM, New York, NY, USA, 13 pages. <https://doi.org/10.1145/3664647.3681089>

1 Introduction

The wide spread of fake news has become an important social issue, posing threats to politics [14], finance [13], and public health [44]. Misusing advanced generative models [9–11, 19, 30] to create misinformation further exacerbates these issues, manifested in the rise of both text fake news [57] and also visual deepfakes [69]. Furthermore, multimodal forgery media through convergence disseminates more expansive information with greater impact to mislead readers. Detecting such fake news poses a unique challenge due to the existence of manipulations in both image and text modalities.

Faced with this challenge, current multimodal fake news detection (MFND) methods [49, 54, 66] primarily focus on incorporating cross-modal features. While some progress has been made, the acquisition of broad world information remains challenging due to the confinement of training to given domains (i.e., closed systems). However, open-world fake news exhibits substantial distribution discrepancies [72], termed domain shift [45, 73], which is manifested in abundant forgery methods and diverse real-world context. The existence of domain shift increases the difficulty of understanding and characterizing open-world fake news in MFND tasks.

To address this problem, we propose to leverage Large Vision-Language Models (LVLMS) [36, 71] which possess rich world knowledge for fake news detectors. This knowledge encompasses a wide array of world facts [4] about public celebrities, social events etc, which enables a comprehensive understanding of agnostic fake

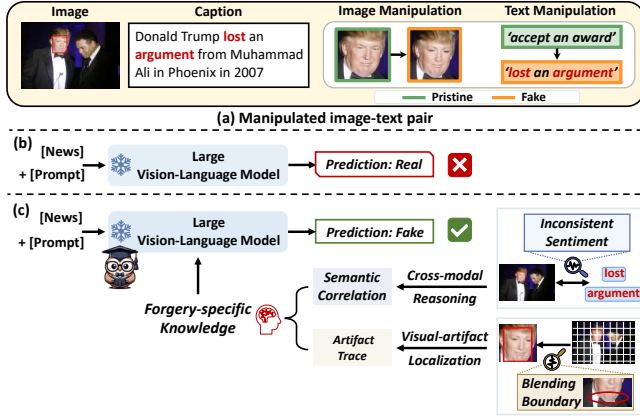


Figure 1: Illustration of the effect of forgery-knowledge augmentation. (a) An example of a manipulated image-text pair in which Trump’s face is swapped with another person and the positive words “accept an award” is replaced with the negative “lost an argument”. (b) Existing LVLMs struggle to correctly judge the news veracity. (c) Incorporating forgery-specific knowledge (i.e., semantic correlation and artifact trace) into LVLMs helps the model make accurate predictions.

news. However, despite their proficiency in recognizing common instances, *the performance of applying off-the-shelf LVLMs to the MFND task is not always satisfying*. On the one hand, since LVLMs are not inherently tailored for MFND tasks, they are still challenging to understand and discover the subtle cross-modal differences [39, 48]. For example, in detecting manipulated image-text pair in Fig. 1-(a), the model must discern the sentiment tendencies of both image and text, which are typically not present in LVLMs’ training data. On the other hand, LVLMs lack sensitivity to localized spatial details [67]. As shown in Fig. 1-(a), when swapping Trump’s face with another person, there exists intrinsic image discrepancies between edited regions and pristine backgrounds, which is hard to perceive with existing LVLMs. Therefore, it is important to augment LVLMs with external information, referred to as *forgery-specific knowledge*, which is absent from model parameters yet useful for manipulation reasoning.

We identified two types of forgery-specific knowledge essential for manipulation reasoning [70]: *semantic correlation* and *artifact trace*. Firstly, manipulated media often disrupt the natural coherence between different modalities, resulting in semantic discrepancies [54]. Secondly, alterations in images usually produce distinctive artifact traces, such as irregular blending boundaries and inconsistencies in color sources, among others [58, 64]. As a result, it would be beneficial to incorporate these two types of knowledge into the training and inference of large vision-language models for multimodal fake news detection.

In this paper, we present a novel framework, namely FKA-Owl which augments LVLMs with forgery-specific knowledge to enhance cross-domain performance for multimodal fake news detection. This framework leverages the rich world knowledge of LVLMs, supplementing it with domain-specific knowledge crucial for identifying multimodal fake news. As shown in Fig. 1-(c), to achieve that, we establish representations of the aforementioned two kinds

of forgery-specific knowledge with two specialized modules. The cross-modal reasoning module applies dual cross-attention mechanisms to integrate visual and textual information from frozen encoders, aiming to identify semantic inconsistencies. Meanwhile, the visual-artifact localization module focuses on detecting precise visual artifacts at multiple levels of detail, using sparse bounding boxes and detailed mask regions to trace artifacts. Subsequently, the encoded knowledge representation embeddings are mapped to the language space of LVLMs with projectors. We devise MFND instruction-following data for fine-tuning and employ both candidate answer heuristics and soft prompts to unleash the extensive knowledge of language models.

Our contributions are summarized as follows:

- We pioneer leveraging rich world knowledge from large vision-language models (LVLMs) and enhancing them with forgery-specific knowledge, to tackle the domain shift issue in multimodal fake news detection. Our proposed method, FKA-Owl, serves as a general detector to bridge the gap.
- FKA-Owl augments LVLMs with forgery-specific knowledge for manipulation reasoning. We propose two lightweight modules: the cross-modal reasoning module and the visual-artifact localization module to extract semantic correlations and artifact traces, respectively.
- The extensive experiments demonstrate the effectiveness of our proposed method under multiple cross-domain settings.

2 Related Work

2.1 Fake News Detection

Fake news detection works can be categorized into unimodal (image-based and text-based) and multimodal methods. Image-based method [5, 65] proposes to exploit edited traces to verify the truth of visual content. One group of CNN-based methods focus on the spatial domain to capture artifact traces, such as blending [29], multiple instance learning [31], patch consistency [68], reconstruction [22, 32], and local mining [12]. The other works transformed images into the frequency domain by applying DCT [50], combining phase spectrum [37], and extracting high-frequency noises [41].

Text-based methods primarily delve into various aspects. Ghanem *et al.* [16] proposes to incorporate topic and affective information extracted from text. Some social context-based methods leverage user feedback [43], news environment [56], propaganda techniques [21] and temporal patterns [20]. Recently, Nan *et al.* [45] and Zhu *et al.* [73] all discover the domain shift issue caused by the word frequency and emotion etc, and propose domain gate and domain memory bank to enrich domain information, respectively.

In contrast to unimodal methods, multimodal methods adhere to incorporate cross-modal features to extract semantic representations [23]. Sabir *et al.* [53] and Wang *et al.* [62] both propose to combine with the external knowledge base to provide complementary semantics information. Qi *et al.* [47] proposes to extract visual entities to understand the high-level semantics of news. Co-attention network [63] and contextual attention network [49] are both designed to better fuse textual and visual features. Moreover, Ying *et al.* [66] proposes improved Multi-gate Mixture-of-Expert networks (iMMoE) to refine and fuse features extracted from multiple views. Ambiguity learning [6] and causal reasoning [7] are

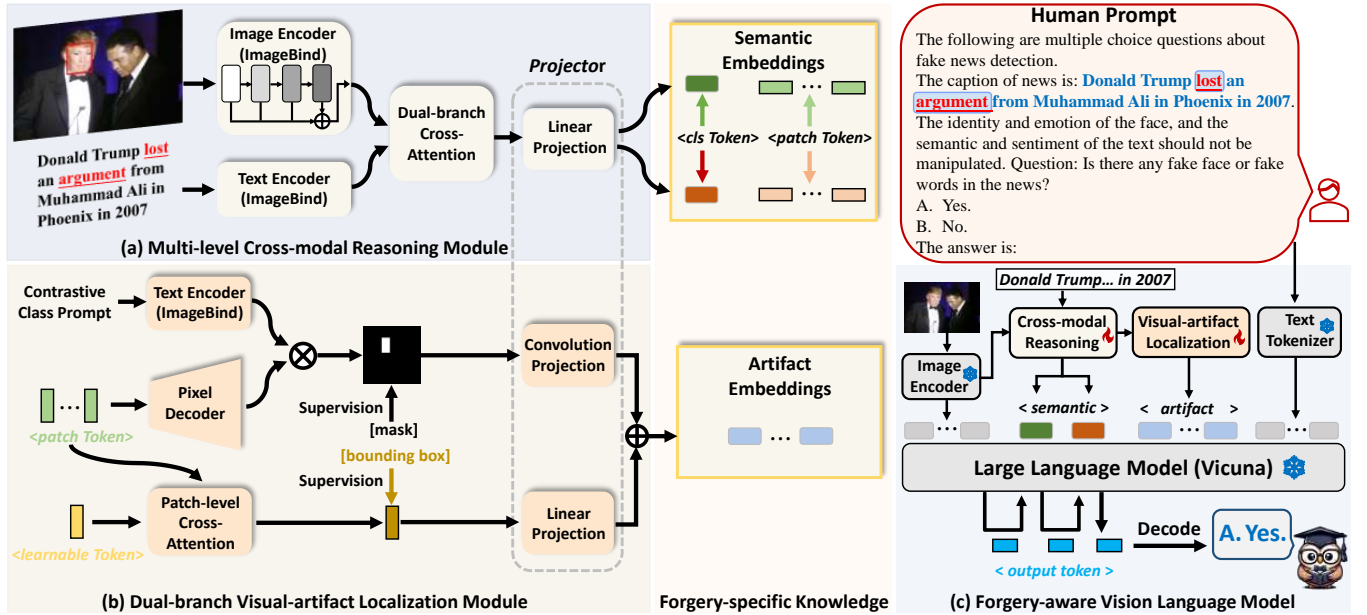


Figure 2: Architecture of our proposed FKA-Owl, which is built upon the off-the-shelf LVLm consisting of an image encoder and the LLM. Given a manipulated image-text pair, the cross-modal reasoning module (a) first extracts cross-modal semantic embeddings and visual patch features. Then, these visual patch features are processed by the visual-artifact localization module (b) to encode precise artifact embeddings. Finally, the semantic and artifact embeddings are incorporated into the forgery-aware vision-language model (c) combined with image features and the human prompt for deep manipulation reasoning.

separately introduced to address the issue of modal disagreement decisions and spurious correlation in data bias. A recent work [54] presents HAMMER, a powerful model that combines contrastive learning and cross-modal aggregation. However, all these methods are typically trained and deployed within closed systems, overlooking the potential benefits of accessing world knowledge.

2.2 Large Vision-Language Models

Large language models (LLMs) such as GPT-3 [3], LLaMA [60] and Vicuna [8], have showcased remarkable performance on various linguistic tasks. More recently, researchers are exploring extending the capability of LLMs to perceive visual signals. LLaVA [36] and Mini-GPT4 [71] first facilitate image-text feature alignment followed by visual instruction tuning. Visual instruction tuning entails additional training of pre-trained models using curated instruction-formatted datasets to enhance models’ generalization to unseen tasks. PandaGPT [59] employs a simple linear layer as a bridge between ImageBind [17] and the Vicuna model, allowing for the multimodal input. The success of LVLms in the general domain has led to the growth of communities such as medical [28], video understanding [25, 38] and image editing [15]. In this work, we leverage the world knowledge inherent in LVLms for a better understanding of open-world fake news.

2.3 Knowledge Augmented Language Models

Utilizing external knowledge to augment language models (LMs) has emerged as a promising solution in knowledge-intensive tasks [26]. One line of works is retrieval-augmented LMs which retrieve relevant passages and incorporate them into LMs. Borgeaud *et*

al. [2] proposes a chunked cross-attention module to incorporate the retrieved text as explicit memory. A lightweight retrieval-augmented dual fine-tuning [34] is introduced to retrofit any LLM. Asai *et al.* [1] introduces self-reflection on retrieved passages to enhance LM’s quality and factuality. Nevertheless, the potential of LVLms augmented with forgery-specific knowledge in multimodal fake news detection remains unexplored.

3 Proposed Method

In this section, we present a unified framework named FKA-Owl which incorporates forgery-specific knowledge into LVLms for manipulation reasoning. We first introduce the overall framework architecture. Then, we elaborate on our proposed multi-level cross-modal reasoning module, dual-branch visual-artifact localization module, and forgery-aware vision-language model. Finally, we detail the loss function for training.

3.1 The Overall Framework

The comprehensive architecture of FKA-Owl is illustrated in Fig. 2. FKA-Owl consists of an image encoder (ImageBind [17]), a cross-modal reasoning module, a visual-artifact localization module, and a large language model (Vicuna [8]). Given a manipulated image-text pair (I, T) , we design two lightweight modules to extract semantic correlations and artifact traces as forgery-specific knowledge representations, respectively. Specifically, the cross-modal reasoning module utilizes dual-branch cross-attention mechanisms to guide cross-modal interactions, facilitating the encoding of semantic embeddings. Concurrently, the visual-artifact localization module gathers local spatial information to establish artifact embeddings

through supervised localization. Then, the forgery-aware vision-language model leverages both the forgery-specific knowledge and inherent world knowledge for deep manipulation reasoning.

3.2 Multi-level Cross-modal Reasoning

The input image and text are encoded first by the frozen pre-trained encoders, denoted as E_v for the image and E_t for the text. Both E_v and E_t originate from the ImageBind, which is aligned with the Vicuna in the off-the-shelf LVM [59]. To obtain both low-level elements and high-level semantic cues, we partition the image encoder into multiple layers with layer index l , enabling the integration of intermediate patch-level features. As shown in Fig. 2-(a), the image features f_v and text features f_t are separately represented as:

$$f_v = \sum_l E_v^l(I), \quad f_t = E_t(T). \quad (1)$$

Both features contain information of object instances within a single modality but lack prior insight into objects referenced by the other modality. This absence of complementary information between modalities may hinder cross-modal semantic reasoning. To this end, we devise the dual-branch cross-attention to guide the interaction between visual and textual features, enabling the extraction of semantic correlations. Attention function [61] is performed on normalized query (Q), key (K), and value (V) features as:

$$\text{Attention}(Q, K, V) = \text{Softmax}\left(\frac{K^T Q}{\sqrt{D}}\right)V. \quad (2)$$

In dual-branch cross-attention, each modal feature (e.g., image) is allowed to serve as queries Q , while keys K and values V can be taken from the other modality (e.g., text):

$$u_v = \text{Attention}(f_v, f_t, f_t), \quad (3)$$

$$u_t = \text{Attention}(f_t, f_v, f_v), \quad (4)$$

where $u_v = \{u_v^{\text{cls}}, u_v^{\text{pat}}\}$, $u_t = \{u_t^{\text{cls}}, u_t^{\text{pat}}\}$. Here, u_v^{cls} and u_t^{cls} are [CLS] tokens from visual/textual embeddings interacted with text/image information. u_v^{pat} and u_t^{pat} are corresponding patch embeddings.

Based on the cross-modal interaction described above, the [CLS] tokens u_v^{cls} and u_t^{cls} can naturally focus on the inter-modal semantic correlations. We concatenate these two [CLS] tokens $\{u_v^{\text{cls}}, u_t^{\text{cls}}\}$ as a joint representation of semantic embedding. Then we use a learnable linear layer to project this generated knowledge into the word embedding space of LVMs, facilitating profound semantic reasoning aided by world factual knowledge.

3.3 Dual-branch Visual-artifact Localization

In addition to extracting semantic correlations between visual and textual features, mining artifact traces is also crucial for distinguishing fake news. Unlike [CLS] token, visual patch tokens with position encoding [61] contain richer local spatial information. Given visual patch tokens u_v^{pat} , we propose a visual-artifact localization module to encode them into artifact embeddings, guided by grounding annotations.

As depicted in Fig. 2-(b), the upper branch which comprises a text encoder and a pixel decoder, is designed to utilize language-driven contrastive learning for pixel-wise localization. Dense features with

good language alignment can provide complementary benefits for fine-grained segmentation [18, 24]. Specifically, two class prompts are initially encoded by the text encoder to obtain corresponding features F_p^i ($i = 1, 2$) $\in \mathbb{R}^{2 \times C_{\text{text}}}$, representing “natural” and “unnatural” states. Detailed contrastive class prompts are presented in the Supplementary Materials. To restore local spatial details, the pixel decoder with consecutive deconvolution layers converts low-resolution features $u_v^{\text{pat}} \in \mathbb{R}^{h \times w \times C_{\text{img}}}$ into high-resolution features $F_h \in \mathbb{R}^{H \times W \times C_{\text{img}}}$. Since patch-level features are not aligned with the textual space, we project both textual features F_p and visual features F_h into a shared representation space. Subsequently, the projected features $\tilde{F}_p \in \mathbb{R}^{2 \times C}$ and $\tilde{F}_h \in \mathbb{R}^{H \times W \times C}$ are employed to compute similarity scores $w \in \mathbb{R}^{H \times W \times 2}$:

$$w^i = \tilde{F}_h \cdot \tilde{F}_p^T, \quad (i = 1, 2). \quad (5)$$

By applying the scores w spatially, we can establish the manipulated segmentation map $M_s \in \mathbb{R}^{H \times W \times 2}$ to achieve per-pixel prediction:

$$M_s^j = \text{softmax}(w) = \log\left(\frac{e^{w^j}}{\sum_{i=1}^2 e^{w^i}}\right), \quad (j = 1, 2). \quad (6)$$

To enrich the representation of artifact traces with multiple levels of details, the lower branch employs multi-head attention for patch-level localization. We utilize a learnable token $q_{\text{tok}} \in \mathbb{R}^{1 \times C_{\text{img}}}$ serving as a query, while visual features u_v^{pat} act as both the key and value. Through the multi-head attention mechanism, local information related to artifacts is aggregated within $u_{\text{agg}} \in \mathbb{R}^{1 \times C_{\text{img}}}$ under the supervision of bounding box grounding:

$$u_{\text{agg}} = \text{Attention}\left(q_{\text{tok}}, u_v^{\text{pat}}, u_v^{\text{pat}}\right). \quad (7)$$

To leverage the artifact knowledge contained in the two-branch features (i.e., the manipulated segmentation map M_s and the aggregated token u_{agg}), we separately devise multiple convolution layers and a simple linear layer as projectors. In this manner, both M_s and u_{agg} are converted into continuous artifact embeddings aligned with the final vision-language model.

3.4 Forgery-aware Vision Language Model

With the extraction of two types of forgery-specific knowledge, merging this external knowledge into LVMs becomes imperative. Both the obtained semantic embeddings and artifact embeddings have been refined to lie in the embedding space for compatibility with language models. Moreover, the introduction of MFND instruction data along with answer heuristics and soft prompts can further activate the capacity of LVMs.

Due to the lack of instruction-follow data in the MFND task, we carefully design an instruction template following the conversational format of the Vicuna model [8], as shown below:

###Human: <ImageFeature><ForgeryFeature>[Human Prompt] ###Assistant:

In this prompt, <ImageFeature> represents the visual tokens produced by the image encoder and <ForgeryFeature> is the combination of semantic and artifact embeddings. The human prompt adopts the multiple choice question answering format, as shown in the dialog box of Fig. 2-(c).

To unleash the potential knowledge of LVLMS in solving MFND tasks, we devise two prompt strategies to serve as more informative inputs in Fig. 2-(c). On the one hand, we utilize candidate answer heuristics [52, 55] to present both the question and answer options to LVLMS and make them predict the symbol (e.g., “A”) associated with the selected answer. This approach enables the language models to explicitly compare different candidate answers showcasing more accurate responses. On the other hand, we implement soft prompt tuning to introduce learnable continuous vectors while freezing the language models. These vectors combined with semantic embeddings facilitate the extraction of additional semantic information. Meanwhile, this approach reduces the burden of LVLMS to learn forgery-aware alignment, thereby mitigating the catastrophic forgetting problem.

3.5 Loss Function

Two groups of loss functions are employed in our training procedure: cross-entropy loss, and two-branch localization losses.

3.5.1 Cross-entropy Loss. In the training of language models, cross-entropy loss is employed to measure the disparity between the text sequence predicted by the models and the target text sequence. The formula is computed according to:

$$\mathcal{L}_{ce} = - \sum_{i=1}^n y_i \log(p_i), \quad (8)$$

where n denotes the token count, y_i is the true label for token i and p_i is the corresponding predicted probability.

3.5.2 Dual-branch Localization Loss. Two-branch localization losses are designed for the precise encoding of artifact traces guided by pixel-wise and patch-level localization, respectively. Pixel-wise localization introduces focal loss [33] and dice loss [42] to enable supervision for the manipulated segmentation map M_S : $\mathcal{L}_{pixel} = \mathcal{L}_{focal} + \mathcal{L}_{dice}$. Patch-level localization involves regressing the final bounding box with the aggregated token u_{agg} and computing the regression losses with the ground-truth box by introducing L1 loss and GIoU loss [51]: $\mathcal{L}_{patch} = \mathcal{L}_{L1} + \mathcal{L}_{giou}$. More details about localization losses are provided in the Supplementary Materials.

Finally, the overall loss function is defined as:

$$\mathcal{L} = \mathcal{L}_{ce} + \mathcal{L}_{pixel} + \mathcal{L}_{patch}. \quad (9)$$

4 Experiments

In this section, we first introduce the overall experimental setup and then provide comprehensive experimental results to demonstrate the superiority of our proposed method.

4.1 Experimental Setup

4.1.1 Dataset. We evaluate the proposed method on DGM⁴ dataset¹ [54] and NewsCLIPPings dataset² [40].

DGM⁴. DGM⁴ dataset is the recently released large-scale multimodal manipulation dataset which comprises 230K image-text paired samples with over 77K pristine pairs and 152K manipulated

Table 1: The statistics of the four subsets within the DGM⁴ dataset categorized by the news sources.

Domain		BBC	Guardian	USA	Wash.
Train	# Real	20436	55459	15472	12725
	# Fake	20375	54244	16339	13134
	Total	40811	109703	31811	25859
Test	# Real	3156	9109	2533	2078
	# Fake	6214	17919	5393	4303
	Total	9370	27028	7926	6381

pairs. In the DGM⁴ dataset, image manipulation involves face swapping and facial emotion editing while text manipulation includes sentence replacement and textual sentiment editing. The construction of the DGM⁴ dataset is based on the VisualNews dataset [35], which is collected from multiple news agencies. Different agencies cover diverse regional perspectives, thematic focus, and language styles (see Supplementary Materials for the analysis of word clouds), resulting in substantial distribution discrepancies. To simulate the open-world domain-shift scenarios, we partition the DGM⁴ dataset into four subsets based on news sources: BBC, The Guardian, USA TODAY (USA), and The Washington Post (Wash.). The statistics of four subsets are listed in Table 1.

NewsCLIPPings. The NewsCLIPPings dataset is the largest real-world multimodal fake news detection benchmark. Forgery samples within this dataset are automatically created by retrieving out-of-context images that appear convincing for a given caption yet display inconsistencies in entities or semantic context. We follow the official dataset partition to report the results on the Merged/Balance subset which has a balanced proportion of different retrieval strategies and positive/negative samples. For our task, we only use the test set data for the cross-dataset evaluation.

4.1.2 Evaluation Metrics. We treat the multimodal fake news detection problem as a binary classification task. Following previous works [46, 54], we apply the Area Under the Receiver Operating Characteristic Curve (AUC), Equal Error Rate (EER), the Accuracy Score (ACC) as our evaluation metrics.

4.1.3 Baselines. The proposed FKA-Owl is compared with the following strong baseline models: **1) PandaGPT** [59]: The off-the-shelf PandaGPT model effectively aligns visual features with the text space of LLMs, enabling it to perform complex multimodal tasks in a zero-shot manner. **2) PandaGPT+SPT**: This model integrates PandaGPT with soft prompt tuning [27] by using the predefined question prompt along with learnable continuous vectors to fine-tune the LVLMS during the instruction tuning phase. **3) HAMMER** [54]: HAMMER employs two unimodal encoders to encode image and text embeddings with contrastive learning for alignment, and then summarize multimodal information through the multimodal aggregator.

4.1.4 Implementation Details. We utilize the visual encoder and text encoder sourced from ImageBind-Huge [17] as the backbone for our image and text feature extractors. Moreover, we employ Vicuna-7B [8] as the inferential LLM, connected through a linear

¹<https://github.com/rshaojimmy/MultiModal-DeepFake>

²https://github.com/g-luo/news_clippings

Table 2: Single-domain performance (%) comparison of baseline models on DGM⁴ dataset. Specifically, we use one subset for training and the remaining subsets for testing. SPT denotes the utilization of soft prompt tuning. (●) indicates the intra-domain performance. The better results in each group are in boldface.

Train	Method	Test											
		BBC			Guardian			USA			Wash.		
		AUC↑	EER↓	ACC↑	AUC↑	EER↓	ACC↑	AUC↑	EER↓	ACC↑	AUC↑	EER↓	ACC↑
	PandaGPT	49.99	50.06	66.31	49.58	50.19	66.30	49.47	50.37	68.04	49.51	50.47	67.43
BBC	PandaGPT+SPT	54.93	47.01	48.29	53.89	47.23	54.33	51.19	49.72	55.96	52.43	48.07	54.91
	HAMMER	87.35	21.40	79.98	80.82	26.81	76.46	65.16	39.40	69.02	67.01	37.92	68.28
	FKA-Owl	89.61	18.61	81.55	84.95	23.55	77.08	73.10	33.91	70.50	74.81	32.29	71.52
Guardian	PandaGPT+SPT	54.66	46.91	46.04	56.57	45.21	50.37	55.99	45.85	50.41	55.58	46.11	50.15
	HAMMER	73.74	31.53	66.74	93.90	13.38	87.45	65.34	39.61	69.23	63.24	41.17	68.50
	FKA-Owl	82.65	25.11	74.92	93.93	13.38	86.60	74.32	32.65	71.06	73.15	33.13	70.16
USA	PandaGPT+SPT	50.01	50.31	59.12	52.88	47.94	59.49	56.50	45.29	58.98	53.89	47.76	60.27
	HAMMER	68.44	35.32	69.81	74.71	30.46	74.35	85.11	22.68	79.08	81.60	25.17	76.90
	FKA-Owl	74.17	31.23	72.91	78.82	27.63	76.66	89.64	18.69	80.96	87.76	20.25	80.68
Wash.	PandaGPT+SPT	51.22	49.50	53.43	53.03	47.43	55.15	54.67	47.05	54.88	53.93	47.09	56.43
	HAMMER	71.29	33.54	70.59	76.78	29.40	74.21	82.11	25.66	77.35	83.30	24.26	77.64
	FKA-Owl	78.56	28.52	73.47	81.97	25.31	76.29	87.07	21.19	79.06	87.94	19.81	80.16

Table 3: Multiple-domain performance (%) comparison of baseline models on DGM⁴ dataset. Specifically, we use two subsets from the identical country for training and the remaining subsets for testing. SPT denotes the utilization of soft prompt tuning. The better results in each group are in boldface.

Method	BBC & Guardian						USA & Wash.					
	USA			Wash.			BBC			Guardian		
	AUC↑	EER↓	ACC↑	AUC↑	EER↓	ACC↑	AUC↑	EER↓	ACC↑	AUC↑	EER↓	ACC↑
PandaGPT+SPT	50.59	49.56	54.44	51.95	48.68	52.55	52.38	48.09	52.54	51.74	48.75	53.13
HAMMER	63.45	39.81	69.19	62.59	40.34	68.64	73.95	32.48	71.86	80.04	27.54	76.06
FKA-Owl	75.17	33.35	71.42	75.15	32.85	70.52	81.06	26.21	75.26	85.88	22.41	78.87

layer. The model is initialized from the instruction-tuned checkpoint provided by PandaGPT. All training images are resized to 224×224 and subjected to random horizontal flipping, as well as random perturbation techniques such as JPEG compression and Gaussian Blur following [54]. The multi-level patch features are extracted from the 8th, 16th, 24th, and 32nd layers of the image encoder. We set the learning rate as $1.5e-5$ with a batch size of 16 and a maximum of 10 epochs when trained on the BBC subset. Linear warm-up and the one-cycle cosine learning schedule are adopted. All experiments are conducted on four NVIDIA GeForce 3090 GPUs with PyTorch. More details about hyperparameter settings are provided in the Supplementary Materials.

4.2 Performance Comparison

We evaluate the cross-domain performance of our FKA-Owl with baselines in single-domain, multiple-domain, and cross-dataset settings respectively.

4.2.1 Single-domain Setting. Table 2 presents the performance of our method and other baseline models in the challenging scenario where a single domain is available. We randomly select one subset of the DGM⁴ dataset as the source domain for training and the remaining subsets as the target domains for testing. From the results, we make the following observations:

- The performance of the existing MFND method drops significantly when tested on the unknown subsets, which verifies the existence of domain shift caused by the deviation in propagation contents.
- FKA-Owl yields substantial improvement on recent LVLs, PandaGPT, and PandaGPT with soft prompt tuning, in both intra-domain and cross-domain testing. Such huge improvement demonstrates the effectiveness of forgery-specific knowledge augmentation in our framework.
- Compared with the state-of-the-art method, HAMMER, our approach shows more remarkable improvement in cross-domain

Table 4: Cross-dataset performance (%) comparison of baseline models on the NewsCLIPpings dataset when trained on DGM⁴ dataset. Specifically, we use multiple subsets from the DGM⁴ dataset for training and the NewsCLIPpings dataset for testing. The better results in each group are in boldface.

Test	Method	BBC & Guardian			USA & Wash.			Average		
		AUC↑	EER↓	ACC↑	AUC↑	EER↓	ACC↑	AUC↑	EER↓	ACC↑
NewsCLIPpings	PandaGPT+SPT	50.84	49.50	50.22	50.62	49.55	50.33	50.73	49.53	50.28
	HAMMER	55.15	45.95	53.92	57.00	44.85	54.56	56.07	45.40	54.24
	FKA-Owl	56.41	45.36	54.46	59.03	43.31	56.22	57.72	44.34	55.34

Table 5: Ablation study of component modules. We evaluate the AUC (in %), EER (in %), and ACC (in %) of variant models on the remaining three subsets when trained on the BBC subset. ML: the extraction of multi-level patch features in the cross-modal reasoning (CR) module. DB: the extraction of dual-branch artifact features in the visual-artifact (VA) Localization module. Avg. denotes the mean value on the three testing subsets.

Componet Module					Test								
ML&CM	DB&VA	Guardian			USA			Wash.			Avg.		
Reasoning	Localization	AUC↑	EER↓	ACC↑	AUC↑	EER↓	ACC↑	AUC↑	EER↓	ACC↑	AUC↑	EER↓	ACC↑
✓		53.89	47.23	54.33	51.19	49.72	55.96	52.43	48.07	54.91	52.50	48.34	55.07
		83.53	23.95	77.03	67.64	36.45	69.52	70.97	34.60	70.33	74.05	31.67	72.29
	✓	81.79	26.76	73.98	66.59	39.02	65.96	69.60	36.67	67.25	72.66	34.15	69.06
✓	✓	84.95	23.55	77.08	73.10	33.91	70.50	74.81	32.29	71.52	77.62	29.92	73.03
FKA-Owl	w/o ML	81.27	26.70	75.49	65.25	39.71	69.20	68.97	36.54	69.21	71.83	34.32	71.30
	w/o DB (upper)	83.70	23.92	77.29	62.85	40.05	70.00	67.73	36.27	70.49	71.43	33.41	72.59
	w/o DB (lower)	84.12	23.88	76.74	70.37	36.36	69.66	73.50	32.87	70.30	76.00	31.04	72.23

testing. For instance, for models trained on the BBC subset, FKA-Owl achieves a 7.7% increase in AUC when testing on the Washington Post subset. This may be credited to the effective utilization of inherent world knowledge from LVLMS in mitigating distribution discrepancies. The combination of forgery-specific knowledge and world knowledge facilitates profound manipulation reasoning in FKA-Owl.

4.2.2 Multiple-domain Setting. The inclusion of domestic news such as the BBC and The Guardian from British, as well as USA TODAY and The Washington Post from America, increases dataset diversity in practical scenarios. We select two subsets from identical countries for training and the remaining two for testing. The results are summarized in Table 3. Our FKA-Owl exhibits significant superiority over both PandaGPT using soft prompt tuning and HAMMER by a large margin. This reveals the effectiveness of our framework in instance-wise domain generalization guided by world knowledge derived from LVLMS, even when jointly learning multiple source domains.

4.2.3 Cross-dataset Setting. To represent the contextual diversity inherent in real-world multimodal fake news, we select multiple subsets from DGM⁴ belonging to the same country for training and report the performance on the NewsCLIPpings. As shown in Table 4, the performance of all methods notably decreases when performing

cross-dataset testing, which implies that the distribution of different datasets does differ. Furthermore, we can observe that incorporating forgery-specific knowledge into LVLMS markedly improves their ability to detect fake news and consistently surpasses the SOTA model HAMMER, reflecting the generalizability of our approach.

Table 6: Ablation study of prompt strategies. AUC (in %) of variant models is reported on the remaining three subsets when trained on the BBC subset. SPT denotes soft prompt tuning, whereas CAH refers to candidate answer heuristics.

Strategy	Guardian	USA	Wash.	Avg.
w/o SPT	84.76	71.98	74.29	77.01
w/o CAH	83.14	67.38	70.55	73.69
w/o SPT & CAH	83.32	66.12	69.94	73.13
FKA-Owl	84.95	73.10	74.81	77.62

4.3 Ablation Study

We perform several ablation experiments to explore the necessity of the proposed component modules, prompt strategies, and LVLMS knowledge respectively, and analysis of potential module choices.

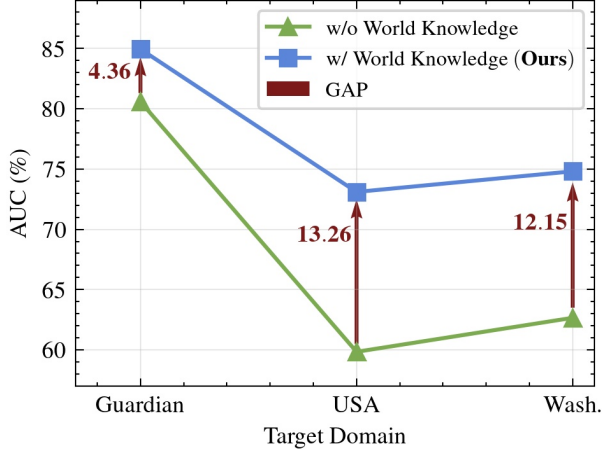


Figure 3: Ablation study of the world knowledge inherent in large vision-language models.

In the following experiments, all ablation results are evaluated on the remaining three subsets when trained on the BBC subset.

4.3.1 The Effect of the Component Modules. In Table 5, we conduct a comprehensive ablation study on the proposed component modules to verify their effectiveness. The first row of Table 5 shows our baseline model that only performs soft prompt tuning, achieving an average AUC of 52.5%. Based on this baseline, we further introduce two separate modules: a multi-level cross-modal (ML&CM) reasoning module and a dual-branch visual-artifact (DB&VA) localization module, with 21.55% and 20.16% improvement in average AUC, respectively. This implies that forgery-specific knowledge augmentation is indispensable for our framework. Comparatively, our model with complete two modules obtains the best performance increasing by 25.12%, indicating the effectiveness and complementarity of these two modules. Moreover, we test the performance of FKA-Owl removing the multi-level features (w/o ML), and FKA-Owl removing any one of the dual-branch features (w/o DB). These variant models lack rich features to represent forgery-specific knowledge leading to a great decrease in cross-domain performance.

4.3.2 The Effect of the Prompt Strategies. The prompt strategies designed in the alignment process and the corresponding results for each case are tabulated in Table 6. First, when removing continuous prompt vectors (w/o SPT), the performance drops a little bit. In addition, after removing the candidate answer options (w/o CAH) in the human instruction prompt, the average performance decreases from 77.62% to 73.69%. In particular, the third row of Table 6 represents that none of both strategies is employed in our proposed framework. Our method substantially outperforms this variant model, implying both two strategies enable the introduction of implicit information to fully activate the capacity of LVLMs.

4.3.3 The Effect of the LVLMs Knowledge. To analyze the impact of world knowledge derived from LVLMs, we compare our method with the common practice of processing fused embeddings in a supervised classification manner [54]. This variant model (w/o World Knowledge) replaces the Vicuna model in FKA-Owl with

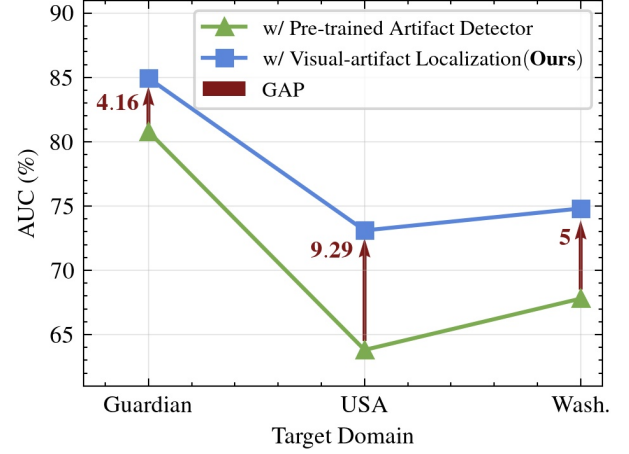


Figure 4: Ablation study of the potential module choice of using pre-trained artifact detector to replace visual-artifact localization module.

a binary classifier to predict true/fake labels. As shown in Fig. 3, harnessing the inherent knowledge in LVLMs improves an average performance by 9.92 points over the variant model. Furthermore, for target domains from distinct countries exhibiting huge distribution differences, FKA-Owl yields more significant improvements in 13.26% and 12.15%. This could be attributed to the fact that world knowledge from LVLMs can effectively guide the representation of agnostic instances.

4.3.4 Analysis on Potential Module Choice. We replace the artifact extractor module in our framework for other design choices. This variant model (w/ Pre-trained Artifact Detector) replaces the visual-artifact localization module in FKA-Owl with the off-the-shelf pre-trained detector [54] to obtain the artifact embeddings. The pre-trained detector employs the ViT backbone with supervised training by grounding annotations. As depicted in Fig. 3, our visual-artifact localization module brings a significant improvement over the variant model. This could be attributed to the fact that Our designed module leverages the intrinsic visual encoder in LVLMs to extract artifact traces, thereby alleviating the burden of aligning forgery-specific knowledge with LVLMs.

5 Conclusion

Our work presents FKA-Owl, a novel framework that leverages rich world knowledge from LVLMs and enhances them with forgery-specific knowledge, to tackle the domain shift issue in multimodal fake news detection. Two types of critical forgery-specific knowledge are augmented in FKA-Owl: semantic correlation between text and images and artifact trace in image manipulation. To inject this knowledge into the LVLM, we first propose two lightweight specialized modules to learn their representations respectively. Then, we transform the generated knowledge into refined embeddings for alignment with language space. The candidate answer heuristics and soft prompts are introduced as supplementary inputs to unleash the extensive knowledge of LVLMs. Extensive experiments verify that FKA-Owl shows superior cross-domain performance compared to the state-of-the-art methods.

Acknowledgments

This research is sponsored by National Natural Science Foundation of China (Grant No. 62306041), Beijing Nova Program (Grant No. Z211100002121106, 20230484488), National Natural Science Foundation of China (No.62176025), National Natural Science Foundation of China (No. U21B2045). This work is partially funded by Youth Innovation Promotion Association CAS (Grant No.2022132), and Beijing Nova Program (20230484276).

References

- [1] Akari Asai, Zeqiu Wu, Yizhong Wang, Avirup Sil, and Hannaneh Hajishirzi. 2024. Self-rag: Learning to retrieve, generate, and critique through self-reflection. In *ICLR*.
- [2] Sebastian Borgeaud, Arthur Mensch, Jordan Hoffmann, Trevor Cai, Eliza Rutherford, Katie Millican, George Bm Van Den Driessche, Jean-Baptiste Lespiau, Bogdan Damoc, Aidan Clark, et al. 2022. Improving language models by retrieving from trillions of tokens. In *ICML*.
- [3] Tom Brown, Benjamin Mann, Nick Ryder, Melanie Subbiah, Jared D Kaplan, Prafulla Dhariwal, Arvind Neelakantan, Pranav Shyam, Girish Sastry, Amanda Askell, et al. 2020. Language models are few-shot learners. In *NeurIPS*.
- [4] Sébastien Bubeck, Varun Chandrasekaran, Ronen Eldan, Johannes Gehrke, Eric Horvitz, Ece Kamar, Peter Lee, Yin Tat Lee, Yuanzhi Li, Scott Lundberg, et al. 2023. Sparks of artificial general intelligence: Early experiments with gpt-4. *arXiv preprint arXiv:2303.12712* (2023).
- [5] Juan Cao, Peng Qi, Qiang Sheng, Tianyun Yang, Junbo Guo, and Jintao Li. 2020. Exploring the role of visual content in fake news detection. *Disinformation, Misinformation, and Fake News in Social Media: Emerging Research Challenges and Opportunities* (2020).
- [6] Yixuan Chen, Dongsheng Li, Peng Zhang, Jie Sui, Qin Lv, Lu Tun, and Li Shang. 2022. Cross-modal ambiguity learning for multimodal fake news detection. In *WWW*.
- [7] Ziwei Chen, Linmei Hu, Weixin Li, Yingxia Shao, and Liqiang Nie. 2023. Causal intervention and counterfactual reasoning for multi-modal fake news detection. In *ACL*.
- [8] Wei-Lin Chiang, Zhuohan Li, Zi Lin, Ying Sheng, Zhanghao Wu, Hao Zhang, Lianmin Zheng, Siyuan Zhuang, Yonghao Zhuang, Joseph E Gonzalez, et al. 2023. Vicuna: An open-source chatbot impressing gpt-4 with 90%* chatgpt quality. See <https://vicuna.lmsys.org> (accessed 14 April 2023).
- [9] Xing Cui, Peipei Li, Zekun Li, Xuannan Liu, Yueying Zou, and Zhaofeng He. 2024. Localize, Understand, Collaborate: Semantic-Aware Dragging via Intention Reasoner. *arXiv preprint arXiv:2406.00432* (2024).
- [10] Xing Cui, Zekun Li, Peipei Li, Yibo Hu, Hailin Shi, and Zhaofeng He. 2023. Chatedit: Towards multi-turn interactive facial image editing via dialogue. In *EMNLP*.
- [11] Xing Cui, Zekun Li, Peipei Li, Huaibo Huang, Xuannan Liu, and Zhaofeng He. 2024. InstaStyle: Inversion Noise of a Stylized Image is Secretly a Style Adviser. In *ECCV*.
- [12] Shichao Dong, Jin Wang, Renhe Ji, Jiajun Liang, Haoqiang Fan, and Zheng Ge. 2023. Implicit Identity Leakage: The Stumbling Block to Improving Deepfake Detection Generalization. In *CVPR*.
- [13] Dina ElBoghdady. 2013. Market quavers after fake AP tweet says Obama was hurt in White House explosions. *The Washington Post* (2013).
- [14] Marc Fisher, John Woodrow Cox, and Peter Hermann. 2016. Pizzagate: From rumor, to hashtag, to gunfire in DC. *The Washington Post* (2016).
- [15] Tsu-Jui Fu, Wenze Hu, Xianzhi Du, William Yang Wang, Yinfei Yang, and Zhe Gan. 2024. Guiding instruction-based image editing via multimodal large language models. In *ICLR*.
- [16] Bilal Ghanem, Simone Paolo Ponzetto, Paolo Rosso, and Francisco Rangel. 2021. FakeFlow: Fake News Detection by Modeling the Flow of Affective Information. In *EACL*.
- [17] Rohit Girdhar, Alaaeldin El-Nouby, Zhuang Liu, Mannat Singh, Kalyan Vasudev Alwala, Armand Joulin, and Ishan Misra. 2023. Imagebind: One embedding space to bind them all. In *CVPR*.
- [18] Zhaopeng Gu, Bingke Zhu, Guibo Zhu, Yingying Chen, Ming Tang, and Jinqiao Wang. 2023. Anomalygpt: Detecting industrial anomalies using large vision-language models. In *AAAI*.
- [19] Jonathan Ho, Ajay Jain, and Pieter Abbeel. 2020. Denoising diffusion probabilistic models. In *NeurIPS*.
- [20] Beizhe Hu, Qiang Sheng, Juan Cao, Yongchun Zhu, Danding Wang, Zhengjia Wang, and Zhiwei Jin. 2023. Learn over Past, Evolve for Future: Forecasting Temporal Trends for Fake News Detection. In *ACL*.
- [21] Kung-Hsiang Huang, Kathleen R. McKeown, Preslav Nakov, Yejin Choi, and Heng Ji. 2023. Faking Fake News for Real Fake News Detection: Propaganda-Loaded Training Data Generation. In *ACL*.
- [22] Yihao Huang, Felix Juefei-Xu, Run Wang, Qing Guo, Lei Ma, Xiaofei Xie, Jianwen Li, Weikai Miao, Yang Liu, and Geguang Pu. 2020. Fakepolisher: Making deepfakes more detection-evasive by shallow reconstruction. In *ACM MM*.
- [23] Ayush Jaiswal, Ekraam Sabir, Wael AbdAlmageed, and Premkumar Natarajan. 2017. Multimedia semantic integrity assessment using joint embedding of images and text. In *ACM MM*.
- [24] Jongheon Jeong, Yang Zou, Taewan Kim, Dongqing Zhang, Avinash Ravichandran, and Onkar Dabeer. 2023. Winclip: Zero-/few-shot anomaly classification and segmentation. In *CVPR*.
- [25] Peng Jin, Ryuichi Takanobu, Caiwan Zhang, Xiaochun Cao, and Li Yuan. 2024. Chat-univi: Unified visual representation empowers large language models with image and video understanding. In *CVPR*.
- [26] Minki Kang, Seanie Lee, Jinheon Baek, Kenji Kawaguchi, and Sung Ju Hwang. 2024. Knowledge-augmented reasoning distillation for small language models in knowledge-intensive tasks. In *Advances in Neural Information Processing Systems*.
- [27] Brian Lester, Rami Al-Rfou, and Noah Constant. 2021. The Power of Scale for Parameter-Efficient Prompt Tuning. In *EMNLP*.
- [28] Chunyuan Li, Cliff Wong, Sheng Zhang, Naoto Usuyama, Haotian Liu, Jianwei Yang, Tristan Naumann, Hoifung Poon, and Jianfeng Gao. 2024. Llava-med: Training a large language-and-vision assistant for biomedicine in one day. In *NeurIPS*.
- [29] Lingzhi Li, Jianmin Bao, Ting Zhang, Hao Yang, Dong Chen, Fang Wen, and Baining Guo. 2020. Face x-ray for more general face forgery detection. In *CVPR*.
- [30] Peipei Li, Rui Wang, Huaibo Huang, Ran He, and Zhaofeng He. 2023. Pluralistic aging diffusion autoencoder. In *ICCV*.
- [31] Xiaodan Li, Yining Lang, Yuefeng Chen, Xiaofeng Mao, Yuan He, Shuhui Wang, Hui Xue, and Quan Lu. 2020. Sharp multiple instance learning for deepfake video detection. In *ACM MM*.
- [32] Jiahao Liang, Huafeng Shi, and Weihong Deng. 2022. Exploring disentangled content information for face forgery detection. In *ECCV*.
- [33] Tsung-Yi Lin, Priya Goyal, Ross Girshick, Kaiming He, and Piotr Dollár. 2017. Focal loss for dense object detection. In *ICCV*.
- [34] Xi Victoria Lin, Xilun Chen, Mingda Chen, Weijia Shi, Maria Lomeli, Rich James, Pedro Rodriguez, Jacob Kahn, Gergely Szilvasy, Mike Lewis, et al. 2024. Ra-dit: Retrieval-augmented dual instruction tuning. In *ICLR*.
- [35] Fuxiao Liu, Yinghan Wang, Tianlu Wang, and Vicente Ordonez. 2021. Visual News: Benchmark and Challenges in News Image Captioning. In *EMNLP*.
- [36] Haotian Liu, Chunyuan Li, Qingyang Wu, and Yong Jae Lee. 2023. Visual instruction tuning. In *NeurIPS*.
- [37] Honggu Liu, Xiaodan Li, Wenbo Zhou, Yuefeng Chen, Yuan He, Hui Xue, Weiming Zhang, and Nenghai Yu. 2021. Spatial-phase shallow learning: rethinking face forgery detection in frequency domain. In *CVPR*.
- [38] Tingkai Liu, Yunzhe Tao, Haogeng Liu, Qihang Fan, Ding Zhou, Huaibo Huang, Ran He, and Yang Hongxia. 2024. DeVAn: Dense Video Annotation for Video-Language Models. In *ACL*.
- [39] Xuannan Liu, Zekun Li, Peipei Li, Shuhan Xia, Xing Cui, Linzhi Huang, Huaibo Huang, Weihong Deng, and Zhaofeng He. 2024. MMFakeBench: A Mixed-Source Multimodal Misinformation Detection Benchmark for LVLMS. *arXiv preprint arXiv:2406.08772* (2024).
- [40] Grace Luo, Trevor Darrell, and Anna Rohrbach. 2021. Newsclippings: Automatic generation of out-of-context multimodal media. In *EMNLP*.
- [41] Yuchen Luo, Yong Zhang, Junchi Yan, and Wei Liu. 2021. Generalizing face forgery detection with high-frequency features. In *CVPR*.
- [42] Fausto Milletari, Nassir Navab, and Seyed-Ahmad Ahmadi. 2016. V-net: Fully convolutional neural networks for volumetric medical image segmentation. In *3D V*.
- [43] Erxue Min, Yu Rong, Yatao Bian, Tingyang Xu, Peilin Zhao, Junzhou Huang, and Sophia Ananiadou. 2022. Divide-and-conquer: Post-user interaction network for fake news detection on social media. In *WWW*.
- [44] Salman Bin Naeem and Rubina Bhatti. 2020. The Covid-19 'infodemic': a new front for information professionals. *Health Information & Libraries Journal* (2020).
- [45] Qiong Nan, Juan Cao, Yongchun Zhu, Yanyan Wang, and Jintao Li. 2021. MD-FEND: Multi-domain fake news detection. In *CIKM*.
- [46] Qiong Nan, Danding Wang, Yongchun Zhu, Qiang Sheng, Yuhui Shi, Juan Cao, and Jintao Li. 2022. Improving Fake News Detection of Influential Domain via Domain-and Instance-Level Transfer. In *COLING*.
- [47] Peng Qi, Juan Cao, Xirong Li, Huan Liu, Qiang Sheng, Xiaoyue Mi, Qin He, Yongbiao Lv, Chenyang Guo, and Yingchao Yu. 2021. Improving fake news detection by using an entity-enhanced framework to fuse diverse multimodal clues. In *ACM MM*.
- [48] Peng Qi, Zehong Yan, Wynne Hsu, and Mong Li Lee. 2024. SNIFFER: Multimodal Large Language Model for Explainable Out-of-Context Misinformation Detection. In *CVPR*.
- [49] Shengsheng Qian, Jinguang Wang, Jun Hu, Quan Fang, and Changsheng Xu. 2021. Hierarchical multi-modal contextual attention network for fake news detection. In *SIGIR*.
- [50] Yuyang Qian, Guojun Yin, Lu Sheng, Zixuan Chen, and Jing Shao. 2020. Thinking in frequency: Face forgery detection by mining frequency-aware clues. In *ECCV*.

- [51] Hamid Rezatofighi, Nathan Tsoi, JunYoung Gwak, Amir Sadeghian, Ian Reid, and Silvio Savarese. 2019. Generalized intersection over union: A metric and a loss for bounding box regression. In *CVPR*.
- [52] Joshua Robinson and David Wingate. 2022. Leveraging Large Language Models for Multiple Choice Question Answering. In *ICLR*.
- [53] Ekraam Sabir, Wael AbdAlmageed, Yue Wu, and Prem Natarajan. 2018. Deep multimodal image-repurposing detection. In *ACM MM*.
- [54] Rui Shao, Tianxing Wu, and Ziwei Liu. 2023. Detecting and grounding multimodal media manipulation. In *CVPR*.
- [55] Zhenwei Shao, Zhou Yu, Meng Wang, and Jun Yu. 2023. Prompting large language models with answer heuristics for knowledge-based visual question answering. In *CVPR*.
- [56] Qiang Sheng, Juan Cao, Xueyao Zhang, Rundong Li, Danding Wang, and Yongchun Zhu. 2022. Zoom Out and Observe: News Environment Perception for Fake News Detection. In *ACL*.
- [57] Qiang Sheng, Juan Cao, Xueyao Zhang, Xirong Li, and Lei Zhong. 2021. Article reranking by memory-enhanced key sentence matching for detecting previously fact-checked claims. In *ACL-IJCNLP*.
- [58] Kaede Shiohara and Toshihiko Yamasaki. 2022. Detecting deepfakes with self-blended images. In *CVPR*.
- [59] Yixuan Su, Tian Lan, Huayang Li, Jialu Xu, Yan Wang, and Deng Cai. 2023. Pandagpt: One model to instruction-follow them all. *arXiv preprint arXiv:2305.16355* (2023).
- [60] Hugo Touvron, Thibaut Lavril, Gautier Izacard, Xavier Martinet, Marie-Anne Lachaux, Timothée Lacroix, Baptiste Rozière, Naman Goyal, Eric Hambro, Faisal Azhar, et al. 2023. Llama: Open and efficient foundation language models. *arXiv preprint arXiv:2302.13971* (2023).
- [61] Ashish Vaswani, Noam Shazeer, Niki Parmar, Jakob Uszkoreit, Llion Jones, Aidan N Gomez, Łukasz Kaiser, and Illia Polosukhin. 2017. Attention is all you need. In *NeurIPS*.
- [62] Youze Wang, Shengsheng Qian, Jun Hu, Quan Fang, and Changsheng Xu. 2020. Fake news detection via knowledge-driven multimodal graph convolutional networks. In *ICMR*.
- [63] Yang Wu, Pengwei Zhan, Yunjian Zhang, Liming Wang, and Zhen Xu. 2021. Multimodal fusion with co-attention networks for fake news detection. In *Findings of ACL-IJCNLP*.
- [64] Yuting Xu, Gengyun Jia, Huaibo Huang, Junxian Duan, and Ran He. 2021. Visual-semantic transformer for face forgery detection. In *IJCB*.
- [65] Puning Yang, Huaibo Huang, Zhiyong Wang, Aijing Yu, and Ran He. 2022. Confidence-Calibrated Face Image Forgery Detection with Contrastive Representation Distillation. In *ACCV*.
- [66] Qichao Ying, Xiaoxiao Hu, Yangming Zhou, Zhenxing Qian, Dan Zeng, and Shiming Ge. 2023. Bootstrapping Multi-view Representations for Fake News Detection. In *AAAI*.
- [67] Yuqian Yuan, Wentong Li, Jian Liu, Dongqi Tang, Xinjie Luo, Chi Qin, Lei Zhang, and Jianke Zhu. 2024. Osprey: Pixel Understanding with Visual Instruction Tuning. In *CVPR*.
- [68] Tianchen Zhao, Xiang Xu, Mingze Xu, Hui Ding, Yuanjun Xiong, and Wei Xia. 2021. Learning self-consistency for deepfake detection. In *ICCV*.
- [69] Tianfei Zhou, Wenguan Wang, Zhiyuan Liang, and Jianbing Shen. 2021. Face forensics in the wild. In *CVPR*.
- [70] Chenguang Zhu, Yichong Xu, Xiang Ren, Bill Yuchen Lin, Meng Jiang, and Wenhao Yu. 2022. Knowledge-Augmented Methods for Natural Language Processing. In *ACL*.
- [71] Deyao Zhu, Jun Chen, Xiaoqian Shen, Xiang Li, and Mohamed Elhoseiny. 2023. Minigpt-4: Enhancing vision-language understanding with advanced large language models. *arXiv preprint arXiv:2304.10592* (2023).
- [72] Yongchun Zhu, Qiang Sheng, Juan Cao, Shuokai Li, Danding Wang, and Fuzhen Zhuang. 2022. Generalizing to the future: Mitigating entity bias in fake news detection. In *SIGIR*.
- [73] Yongchun Zhu, Qiang Sheng, Juan Cao, Qiong Nan, Kai Shu, Minghui Wu, Jindong Wang, and Fuzhen Zhuang. 2022. Memory-guided multi-view multi-domain fake news detection. *TKDE* (2022).

FKA-Owl: Advancing Multimodal Fake News Detection through Knowledge-Augmented LVLMS

Supplementary Material

A Contrastive Class Prompts

Fig. A5 presents a detailed list of prompts utilized for implementing the contrastive class prompt. Following WinCLIP [24], we employ the compositional prompt ensemble to generate texts representing natural and unnatural states. Specifically, we curate prompt templates involving *a photo of a* [c] and *a photo of the* [c]. A complete prompt can be composed by replacing the token [c] in the template-level prompt with one of the state-level prompts, either from the natural or unnatural states.

Template-level Prompt:	
(1) <i>a photo of a</i> [c]	(2) <i>a photo of the</i> [c]

State-level Prompt:	
(a) State-level (natural)	(b) State-level (unnatural)
<ul style="list-style-type: none"> c := "object" c := "natural object" c := "genuine object" c := "realistic object" c := "object without blending boundaries" c := "object without inconsistent textures" c := "object without unnatural shadows" 	<ul style="list-style-type: none"> c := "unnatural object" c := "synthetic object" c := "unrealistic object" c := "object with blending boundaries" c := "object with inconsistent textures" c := "object with unnatural shadows"

Figure A5: Lists of two state-level prompts considered in this paper to construct contrastive class prompts.

B Localization Loss

B.1 Pixel-wise Localization Loss

The manipulated segmentation map M_s is utilized to calculate focal loss [33] and dice loss [42] supervised by the grounding mask. In the multimodal fake news detection task, where the majority of regions in fake images remain pristine, employing focal loss can alleviate the issue of class imbalance. The Focal loss is computed as follows:

$$\mathcal{L}_{\text{focal}} = -\frac{1}{n} \sum_{i=1}^n (1 - p_i)^\gamma \log(p_i), \quad (10)$$

where n denotes the total number of pixels, p_i represents the predicted probability of positive classes, and γ is a hyperparameter for adjusting the weight of hard-to-classify samples. In our implementation, we set γ to 2.

Dice loss is based on the dice coefficient and can be computed as follows:

$$\mathcal{L}_{\text{dice}} = 1 - \frac{2 \sum_{i=1}^n y_i \hat{y}_i}{\sum_{i=1}^n y_i^2 + \sum_{i=1}^n \hat{y}_i^2}, \quad (11)$$

where n denotes the total number of pixels, y_i is the pixel value in the segmentation map and \hat{y}_i is the ground truth value.

B.2 Path-level Localization Loss

To regress the predicted bounding box, the aggregated token u_{agg} is fed into the BBox Detector D_o , which comprises two multi-layer

perception (MLP) layers. Then we compute the patch-level Localization loss by combining normal L1 loss and generalized Intersection over Union (IoU) loss as follows:

$$\begin{aligned} \hat{b} &= D_o(u_{\text{agg}}), \\ \mathcal{L}_{\text{patch}} &= \mathcal{L}_{L_1}(b, \hat{b}) + \mathcal{L}_{\text{giou}}(b, \hat{b}), \end{aligned} \quad (12)$$

where \hat{b} denote the predicted bounding boxes and b denote the ground-truth box.

C Real-world Distribution Divergence

In Fig. C6, we present word clouds to illustrate the distribution divergence in real-world context across regional perspectives and thematic focus. Notably, the BBC predominantly reports British news, encompassing various subjects such as culture and entertainment. Conversely, the Washington Post tends to emphasize American political news. This disparity leads to variations in word usage across distinct domains. For instance, the commonly used words in BBC news include "prime minister", "children", and "family" etc, while in the Washington Post news, prevalent terms are "president", "Donald Trump", and "Obama", etc.

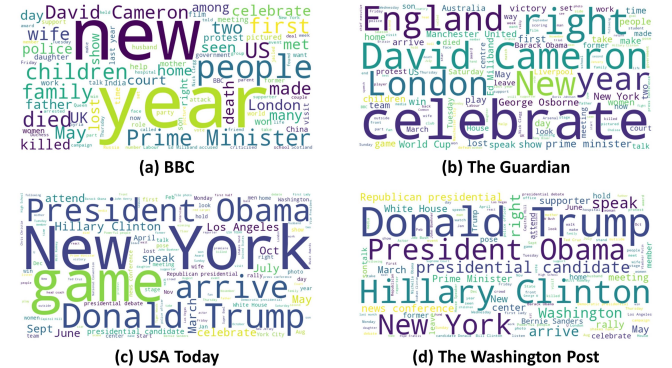





Figure C6: Word clouds of training data sourced from subsets of BBC, The Guardian, USA Today, and The Washington Post, where the size of terms corresponds to the word frequency.

D Implementation Details

Here we provide detailed implementation details for training on the remaining three subsets: The Guardian, USA TODAY, and The Washington Post. The hyperparameters are the same for all subsets but differentiate the learning rate, batch size, and maximum epoch by dataset scale, detailed in Table D7. Additionally, to ensure a fair comparison, the hyperparameters for the PandaGPT using soft prompt tuning are set to be consistent with the values used in our method. For the state-of-the-art method HAMMER, the hyperparameters are set to default values used in [54].

Case 1: When confronting multimodal pristine news, FKA-Owl predicted correctly, while the vanilla LVLM did incorrectly.

 <p><i>Um Jaafar a woman fighter in the Free Syrian Army sits with her husband Abu Jaafar a Sawt alHaq</i></p> <p>GT: True PandaGPT Pred: Fake FKA-Owl Pred: True</p>	 <p><i>Erin Meredith and Addison talk over dinner</i></p> <p>GT: True PandaGPT Pred: Fake FKA-Owl Pred: True</p>	 <p><i>While on his regular patrol Officer Robert Grisby listens to details of a family dispute in Cincinnati's OvertheRhine neighborhood</i></p> <p>GT: True PandaGPT Pred: Fake FKA-Owl Pred: True</p>
--	---	---

Case 2: When confronting multimodal fake news, both FKA-Owl and vanilla LVLM predicted correctly.




 <p><i>Social commentators have called on Narendra Modi to rein in hardline Hindu groups</i></p> <p>GT: Fake PandaGPT Pred: Fake FKA-Owl Pred: Fake</p>	 <p><i>trump has been talking about the muslim problem for years</i></p> <p>GT: Fake PandaGPT Pred: Fake FKA-Owl Pred: Fake</p>	 <p><i>Clinton and Kaine celebrate while waving to the crowd at the Florida campaign event</i></p> <p>GT: Fake PandaGPT Pred: Fake FKA-Owl Pred: Fake</p>
---	---	---

Figure E7: Cases in the testing set where vanilla LVLM and FKA-Owl confront with pristine news and fake news. (●) indicates wrong prediction and (●) indicates correct prediction.

Table D7: Hyperparameters used in The Guardian, USA TODAY, and The Washington Post subsets.

Parameters	Train set		
	Guardian	USA	Wash.
Optimizer	AdamW	AdamW	AdamW
Learning Rate	4.1e-5	1.1e-5	1e-5
LR Scheduler	Linear	Linear	Linear
Batch Size	128	16	16
Maximum Epoch	12	10	10

E Case Analysis

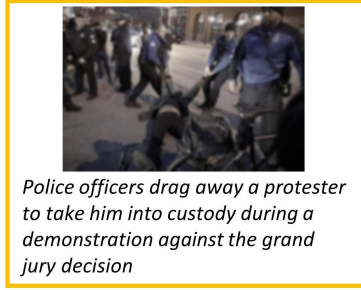
Fig. E7 and Fig. E8 depict cases from the testing set. The former illustrates comparisons between the vanilla LVLM and FKA-Owl, while

the latter showcases cases where either the compared methods or the LVLM using soft prompt tuning predictions are incorrect.

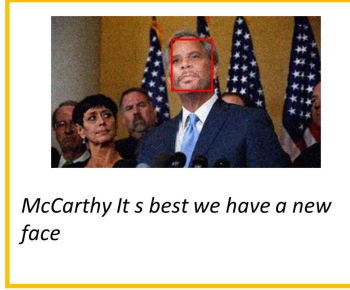
In Fig. E7, Case 1 and Case 2 show cases where the vanilla LVLM model predicts all labels as “Fake” while the FKA-Owl makes correct predictions. This implies that the vanilla LVLM lacks the necessary knowledge to effectively detect fake news when learning from the general corpus, making it challenging to accurately characterize the concept of forgery and provide precise responses. Consequently, the vanilla LVLM relies heavily on common prompt words, such as “face”, resulting in all labels being predicted as “Fake”.

Figure E8 illustrates comparisons between our method with the state-of-the-art model HAMMER, and PandaGPT using soft prompt tuning (PandaGPT+SPT). In Case 3, the absence of forgery-specific knowledge impedes the ability of PandaGPT to perform manipulation reasoning, especially when confronted with fake images containing subtle artifacts. In Case 4, the powerful model HAMMER struggles to handle agnostic instances due to the lack of prior

Case 3: Both HAMMER and FKA-Owl predicted correctly, while the LVLMS using soft prompt tuning did incorrectly.



GT: True
PandaGPT+SPT Pred: **Fake**
HAMMER Pred: **True**
FKA-Owl Pred: **True**



GT: Fake
PandaGPT+SPT Pred: **True**
HAMMER Pred: **Fake**
FKA-Owl Pred: **Fake**



GT: Fake
PandaGPT+SPT Pred: **True**
HAMMER Pred: **Fake**
FKA-Owl Pred: **Fake**

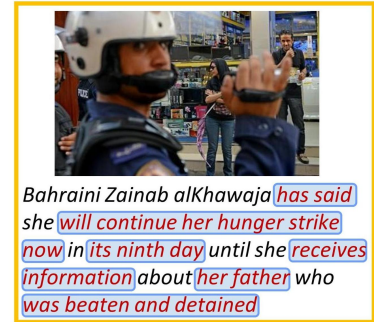
Case 4: Both the LVLMS using soft prompt tuning and FKA-Owl predicted correctly, while HAMMER did incorrectly.



GT: True
PandaGPT+SPT Pred: **True**
HAMMER Pred: **Fake**
FKA-Owl Pred: **True**



GT: Fake
PandaGPT+SPT Pred: **Fake**
HAMMER Pred: **True**
FKA-Owl Pred: **Fake**

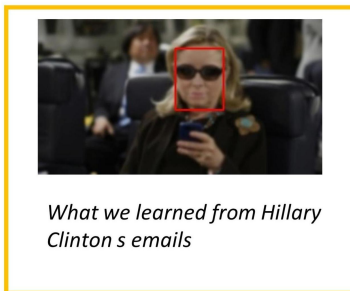


GT: Fake
PandaGPT+SPT Pred: **Fake**
HAMMER Pred: **True**
FKA-Owl Pred: **Fake**

Case 5 : Only FKA-Owl predicted correctly, while HAMMER and the LVLMS using soft prompt tuning did incorrectly.



GT: True
PandaGPT+SPT Pred: **Fake**
HAMMER Pred: **Fake**
FKA-Owl Pred: **True**



GT: Fake
PandaGPT+SPT Pred: **True**
HAMMER Pred: **True**
FKA-Owl Pred: **Fake**



GT: True
PandaGPT+SPT Pred: **Fake**
HAMMER Pred: **Fake**
FKA-Owl Pred: **True**

Figure E8: Cases in the testing set where at least one in the Baseline and the LVLMS using soft prompt tuning made incorrect predictions. (●) indicates wrong prediction and (●) indicates correct prediction.

information, resulting in incorrect judgments regarding unseen fake news. Conversely, Case 5 demonstrates the effectiveness of

our FKA-Owl, which integrates inherent world knowledge from LVLMS and incorporates forgery-specific information to make accurate predictions.